

RESEARCH

Open Access



# Direct RNA sequencing reveals chicken post-transcriptional modifications in response to *Campylobacter jejuni* inoculation

Yanan Zhao<sup>1</sup>, Yuanmei Wang<sup>1</sup>, Yanru Ren<sup>1</sup>, Long Liu<sup>1</sup>, Tianyi Wang<sup>1</sup>, Liying Liu<sup>3</sup> and Xianyao Li<sup>1,2\*</sup>

## Abstract

**Background** *Campylobacter jejuni* (*C. jejuni*), is a leading cause of food-borne pathogen, poses significant threats to poultry industry and public health. Post-transcriptional modifications play crucial roles in regulating the immune system and cell functions. However, the epigenetic regulation in response to *C. jejuni* inoculation in chicken remains elusive.

**Results** The RNA transcriptional profiles and base modification alterations in the chicken cecum following *C. jejuni* inoculation were characterized using direct RNA sequencing and analyzed by bio-informatics and expression analysis. We identified 40,755 transcripts and 23,877 genes following *C. jejuni* inoculation in the chicken cecum. Of which, 10,503 novel transcripts across 8,560 genes were identified. The number of significantly differential alternative splicing events and poly(A) tails was 192 and 426, respectively ( $P < 0.05$ ). Particularly, 121 significantly differentially expressed transcripts which were enriched in defense response to gram-negative bacteria, positive regulation of interleukin-6 production, innate immune response, macrophage activation ( $P < 0.05$ ). Among these, 29 transcripts contained m<sup>5</sup>C sites, and 37 transcripts contained m<sup>6</sup>A sites. The transcripts containing m<sup>6</sup>A/m<sup>5</sup>C modifications displayed higher expression levels and shorter poly(A) tails than those without modifications. Functional analysis of these modules including differentially expressed transcripts (DETs), transcripts with differentially significant poly(A) tail length, m<sup>5</sup>C modified DETs, and m<sup>6</sup>A modified DETs showed that the negative regulation of interferon-beta production was enriched ( $P < 0.05$ ). Specially, ENSGALT00000020390 (novel transcript), and ENSGALT00000053962 (IFIH1-202) were significantly enriched.

**Conclusions** This study provided a post-transcriptional modification profile in the chicken cecum post *C. jejuni* inoculation, including alternative splicing, poly(A) tail length, m<sup>6</sup>A and m<sup>5</sup>C modifications. ENSGALT00000012480 and *IFIH1* could be potential candidate genes as epigenetic markers following *C. jejuni* inoculation. The findings provide new insights into the complexity of expression regulation and data resource of the epitranscriptome, enhancing our understanding on epigenetic modification regulating *C. jejuni* inoculation.

**Keywords** SPF chicken, *Campylobacter jejuni*, Post-transcriptional modifications, N<sup>6</sup>-methyladenosine, Direct RNA sequencing

\*Correspondence:

Xianyao Li  
xyl@sdau.edu.cn

<sup>1</sup>Shandong Provincial Key laboratory for Livestock Germplasm Innovation & Utilization, College of Animal Science and Technology, Shandong Agricultural University, Tai'an 271017, Shandong, China

<sup>2</sup>Key Laboratory of Efficient Utilization of Non-grain Feed Resources (Co-construction by Ministry and Province), Ministry of Agriculture and Rural Affairs, Tai'an 271017, Shandong, China

<sup>3</sup>College of Life Sciences, Shandong Agricultural University, Tai'an 271017, Shandong, China



© The Author(s) 2025. **Open Access** This article is licensed under a Creative Commons Attribution-NonCommercial-NoDerivatives 4.0 International License, which permits any non-commercial use, sharing, distribution and reproduction in any medium or format, as long as you give appropriate credit to the original author(s) and the source, provide a link to the Creative Commons licence, and indicate if you modified the licensed material. You do not have permission under this licence to share adapted material derived from this article or parts of it. The images or other third party material in this article are included in the article's Creative Commons licence, unless indicated otherwise in a credit line to the material. If material is not included in the article's Creative Commons licence and your intended use is not permitted by statutory regulation or exceeds the permitted use, you will need to obtain permission directly from the copyright holder. To view a copy of this licence, visit <http://creativecommons.org/licenses/by-nc-nd/4.0/>.

## Background

*Campylobacter jejuni* (*C. jejuni*) is the leading cause of Campylobacteriosis, which was recognized as the first zoonosis in human [1], typically through contaminated chicken meat and eggs [2]. The chicken cecum is the main colonization site for *C. jejuni* [3]. Intensive researches have confirmed that the high level of cecal colonization usually leads to a high prevalence of the pathogen at the flock level and frequent contamination of carcass during slaughter and processing. And it affects more than 1.3 million people annually in the United States [4, 5].

Post-transcriptional modifications are widespread in eukaryotes and have gained extensive attention due to their major roles in RNA metabolism, immunity, development and disease [6]. The poly(A) tail can cooperate with the 7-methylguanosine cap ( $m^7Gppp$ ) on the 5'-end of the mRNA to stimulate the translation [7]. The poly(A) tail lengths underwent distinctive changes during macrophage activation [8]. Alternative splicing (AS) could generate diverse splice isoforms from a single gene during T cell activation and autoimmune diseases [9, 10]. Recently, aberrant AS events have gained considerable momentum in the pathogenesis of many diseases, such as inflammatory bowel disease (IBD) [11], liver disease [12], and tumor [13]. RNA methylation could be involved in the half life measurements of embryonic stem cells and the process of hot shock stress through regulating mRNA stability, translational efficiency, or gene expression [14, 15].

N6-methyladenosine ( $m^6A$ ) and 5-methylcytosine ( $m^5C$ ) are the most prevalent, reversible and abundant internal RNA modifications in eukaryotic cells [16, 17]. It is reported that  $m^6A$  and  $m^5C$  modifications can regulate the proliferation and differentiation of immune cells at the gene level, thereby affecting the immune system [6]. Chen et al. [18] found that  $m^6A$  and  $m^5C$  modification of GPX4 promotes anticancer immunity via activating the cGAS-STING.  $m^6A$  can reprogram naive T cells for proliferation and differentiation [19]. The deletion of *METTL3* in mouse can inhibit T cell homeostasis and differentiation [20].  $m^5C$  is linked to biological alteration in cells during cancer development [21, 22]. NSUN2, a crucial member of  $m^5C$ , can allow tumor escape from chemotherapy by modulating the Ras signaling pathway [23]. *Campylobacter* inoculation can activate chicken immune system and initiate an inflammatory response [24]. However, the post-transcriptional modification of chicken responding to *C. jejuni* inoculation still remains unclear.

Direct RNA Sequencing (DRS) is able to directly sequence RNA without the need of cDNA sequencing or PCR, which can be used for single-molecule sequencing and direct RNA modifications location analysis [25]. To elucidate the role of chicken post-transcriptional

modification in regulating *C. jejuni* inoculation, we characterized the single-base resolution maps of alternative splicing, poly(A) tail length,  $m^6A$ , and  $m^5C$  modifications of chicken cecum following *C. jejuni* inoculation using DRS. Our results will provide new insights into the functions of specific mRNA levels and post-transcriptional regulation in chicken responding to *C. jejuni* inoculation, and provide innovative strategies for chicken disease-resistance breeding.

## Methods

### Sample collection

In this study, a total of 20 3-day-old specific pathogen free (SPF) White Leghorn chicks were used (Jinan SAIS Poultry Co., Ltd, China). In brief, each chick in the treated group (T group) was orally inoculated with 0.5 mL  $1.65 \times 10^8$  CFU/mL *C. jejuni* solution, and chicks in the control group (C group) were orally inoculated with 0.5 mL sterile PBS solution. Chicks in C and T groups were raised in two separated incubators under the same conditions with free access to sterile feed and water. The cecum rinsed with sterile PBS 3-5 times was collected in 10 individual chicks from each group at 8 hours post *C. jejuni* inoculation (hpi), snap frozen in liquid nitrogen and stored at  $-80^\circ\text{C}$ . All animal procedures were approved by Shandong Agricultural University Animal Care and Use Committee (SDAUA-2019-060).

### RNA extraction, library preparation and sequencing

Total RNA was extracted from each sample using the Total RNA Kit I (OMEGA, US) in accordance with the manufacturer's guideline. The RNA integrity and concentration were measured using Agilent 2100 (Agilent, US) and Nanodrop (Thermo Fisher Scientific, US), respectively. According to the manufacturer's instructions, the total RNA was then purified and concentrated using NEBNext Poly(A) mRNA Magnetic Isolation Module (E7490S, New England Biolabs). Library was constructed for each sample with 20  $\mu\text{g}$  qualified RNA. The library was loaded onto ONT R9.4 flow cells and sequenced on a PromethION sequencer (Oxford Nanopore Technologies, Oxford, UK).

### Reads filtering, mapping, and identifying of the transcripts and novel genes

The raw reads were filtered using NanoFilt (version: 2.6.0) with parameters “-q 7 -l 50” [26]. Short reads less than 50 bp were filtered with the Fclmr2 (version 0.1.2) [27]: based on the quality value of the sequencing data (Default parameter: quality value > 7), reads with a quality value greater than 7 are marked as “pass”, while those with a quality value less than 7 are marked as “fail”. Reads with a quality value lower than 7 will be filtered out. The clean reads were mapped to the chicken reference genome

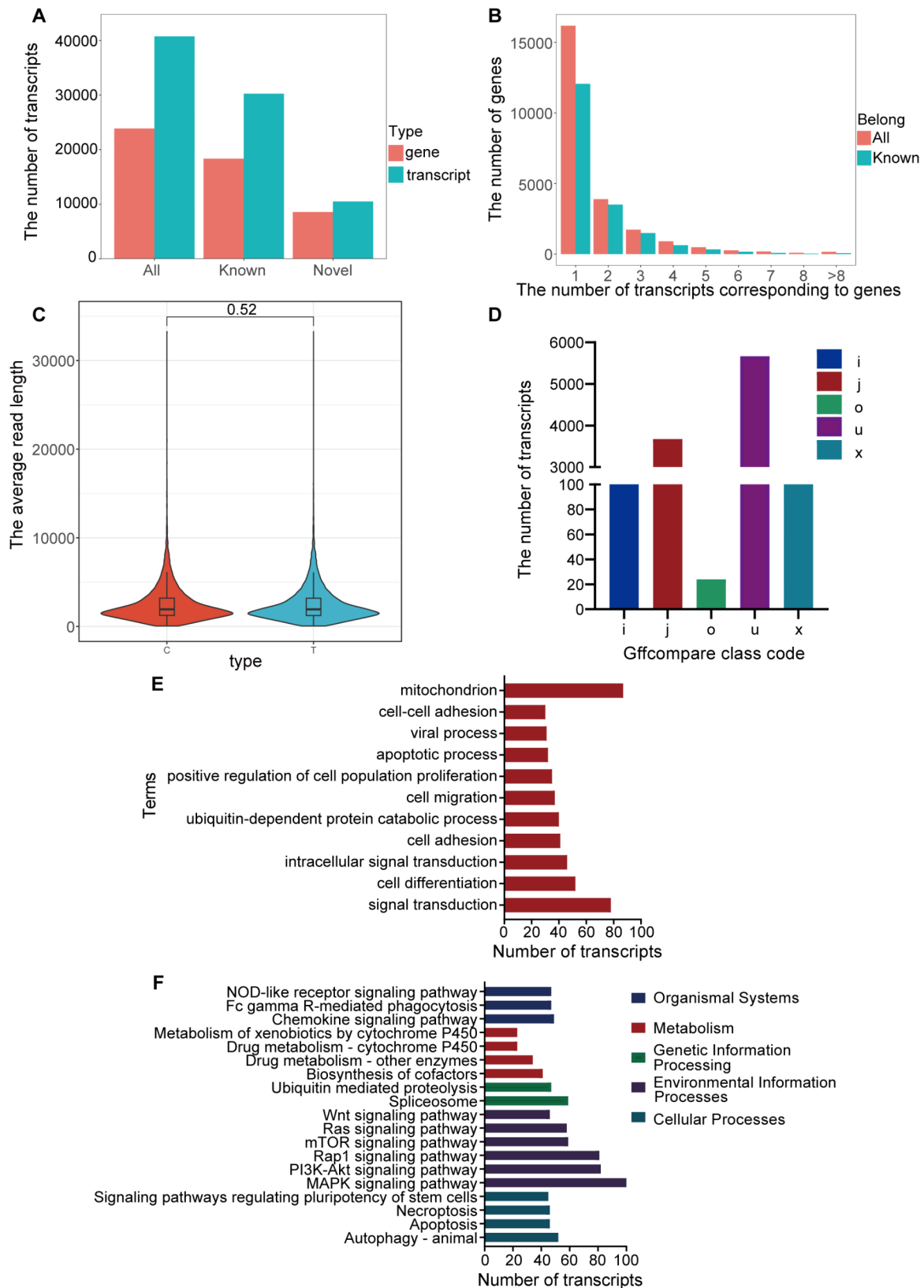


Fig. 1 (See legend on next page.)

(See figure on previous page.)

**Fig. 1** The characterization of genes and transcripts in chicken cecum following *C. jejuni* inoculation. **(A)** The number of genes and transcripts identified by DR. **(B)** Number of transcripts corresponding to genes. **(C)** The read length distribution of transcripts. **(D)** Number of different types of novel transcripts. i, fully contained within a reference intron; j, multi-exon with at least one junction match; o, other same-strand overlapping with reference exons; u, none of the above (unknown, intergenic); and x, exonic overlapping on the opposite strand. **(E)** GO analysis of novel transcripts. **(F)** KEGG annotation and pathway of novel transcripts

(GRCg6a) (<http://genome.ucsc.edu/>) using Minimap2 (version: 2.17-r941) [28] with parameters “-ax splice -uf -k14”. A Flair (version: 1.5.0) [29] with parameters “-t 20” was used to obtain a consensus sequence based on the alignment results. We merged the alignment with only differences in exons at the 5' end and obtained the non-redundant transcript sequence using StringTie (version: 2.1.4) [30], thus producing the novel reference transcript file for the chicken genome. GffCompare (version: 0.12.1) with parameters “R-C-K-M” [31] was used to discover novel transcripts and genes. The quality of sequencing data and reads alignment was in supplemental Table 1.

#### Analysis of differentially expressed transcripts

Salmon 1.4.0 [32] was used to estimate the transcripts expression by calculating Transcripts Per Million (TPM). The differentially expressed transcripts (DETs) were identified with Fold Change > 2 and *P* value < 0.05.

#### Alternative splicing analysis

The transcript was compared to known transcripts of the genome. Suppa2 software [33] (<https://github.com/comp-rna/SUPPA>) was used to obtain the variable splice type and identify the different variable splice between C and T groups with parameters “-f IOE -e se SS MX RI FL”.

#### Characterization of poly(A) tail length

The length of poly(A) was calculated using NanoPolish (version: 0.13.2) with parameters “poly(A)”. Mann Whitney U test was used to test the correlation between the poly(A) length and the expression of transcripts.

#### The identification and calculation of RNA base modification

The m<sup>5</sup>C modifications sites of RNA sequences were identified with Tombo (1.5) with alternative model [34]. The m<sup>5</sup>C modification with fraction > 0.7 and coverage > 10 was selected for further analysis. The nine bases surrounding the modified C were used to analyze the conserved motif using MEME [35]. The m<sup>6</sup>A modifications sites of RNA sequences were identified with Tombo's de novo model and the MINES process (<https://github.com/YeoLab/MINES>). The m<sup>6</sup>A site with fraction > 0.5 and coverage > 10 was selected for further analysis. Methylkit software [36] was used to analyze the differentially methylated sites (DMS).

#### Functional annotation and enrichment analysis

Gene Ontology (GO) and Kyoto Encyclopedia of Genes and Genomes (KEGG) enrichment analysis were performed for DETs using clusterProfiler package [37]. *P* < 0.05 was considered significantly enriched.

#### Quantitative real-time polymerase chain reaction

One ug total RNAs (Note: The batch of RNA used was consistent with that of RNA sequencing) was used for cDNA synthesis using PrimeScript™ RT reagent Kit with gDNA Eraser (Takara, Japan). Quantitative real-time PCR (qRT-PCR) was conducted using SYBR Premix Dimer Eraser (Takara, Japan) and associated primers (Sangon, China). The relative gene expression was calculated using the 2<sup>-ΔΔCt</sup> method. The data were analyzed using the One-way ANOVA. *P* < 0.05 was considered significance. The detailed primer was listed in supplemental Table 2.

## Results

#### Characterization of genes and novel transcripts

We identified 23,877 genes and 40,755 transcripts, including 8,560 novel genes and 10,503 novel transcripts (Fig. 1A). Two thirds of genes (*n* = 16,171) contained one transcript (Fig. 1B). The average read length of transcripts for C and T groups was 2,480.32 and 2,473.20, respectively (Fig. 1C). The number of transcripts with “o” type is the least (*n* = 24), whereas that with “u” type is the highest (*n* = 5,665) (Fig. 1D). The functional annotation of GO and KEGG pathway for the novel transcripts was conducted. In term of GO biological process (BP), signal transduction, cell differentiation, intracellular signal transduction, cell adhesion, cell migration, apoptotic process, viral process, and cell-cell adhesion were enriched (Fig. 1E, Supplemental Table 3A). For KEGG analysis, the novel transcript were significantly enriched in NOD-like receptor signaling pathway, chemokine signaling pathway, Wnt signaling pathway, Ras signaling pathway, mTOR signaling pathway, Rap1 signaling pathway, PI3K-Akt signaling pathway, MAPK signaling pathway, apoptosis, and necroptosis (Fig. 1F, Supplemental Table 3B).

#### The function of differentially expressed transcripts following *C. jejuni* inoculation

There were 121 transcripts (Fold Change > 2, *P* < 0.05) differentially expressed between the treated and control groups, with 59 upregulated and 62 downregulated transcripts in treated group (Fig. 2A). The expression of

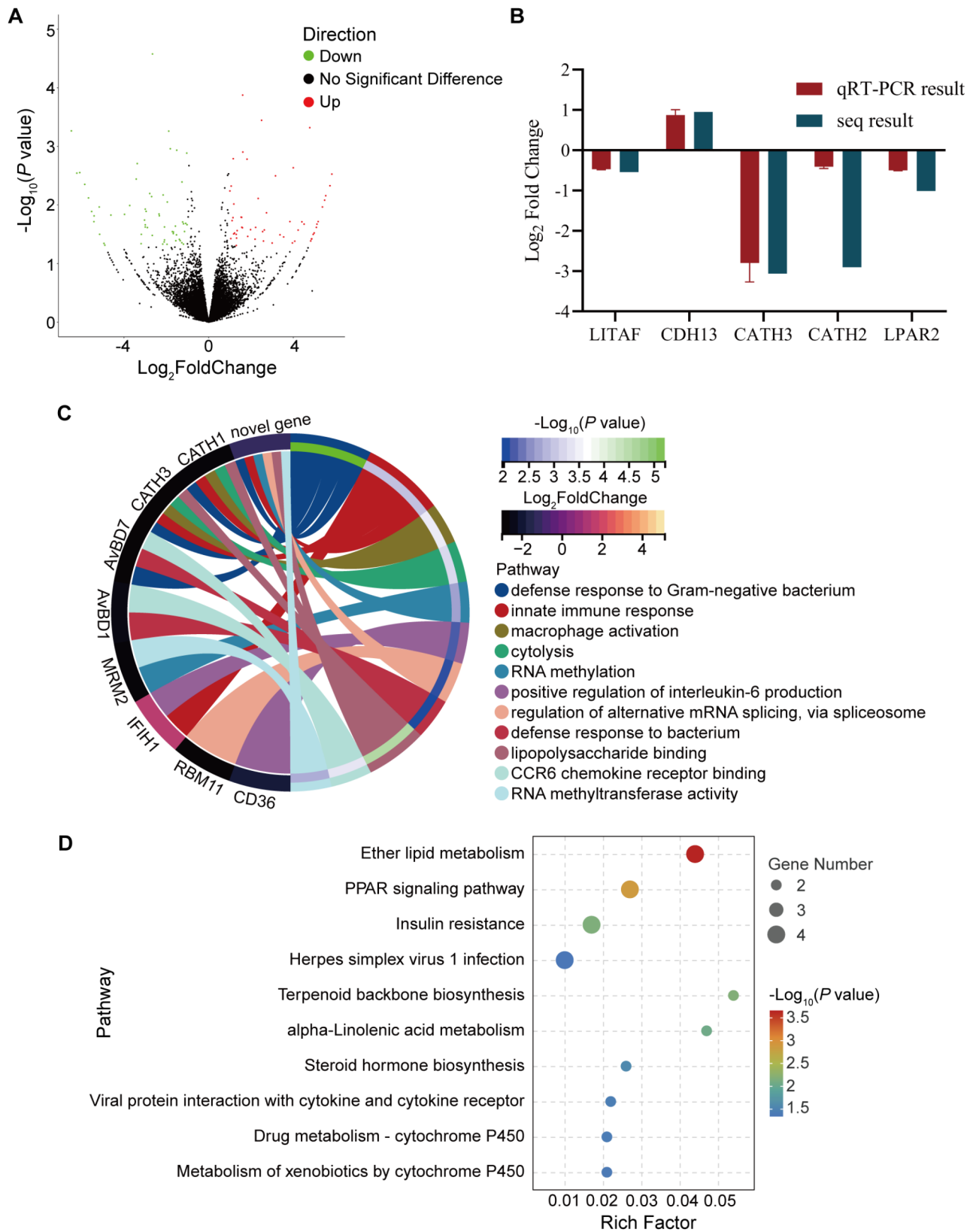


**Fig. 2** The function of differentially expressed transcripts following *C. jejuni* inoculation. **(A)** Volcano plot of the differentially expressed transcripts between C and T groups. **(B)** The accuracy verification result of Direct RNA sequencing (DRS) by qRT-PCR. **(C)** GO analysis of differentially expressed transcripts. **(D)** KEGG pathway of differentially expressed transcripts

5 RT-qPCR validated genes were consistent with those of Direct RNA sequencing (Fig. 2B). Then, we conducted functional annotation of GO and KEGG pathway for these differentially expressed transcripts (DETs) corresponding genes. Those DETs were significantly enriched in 86 GO terms (57 biological process (BP), 23 molecular function (MF), and 6 cellular components (CC)) ( $P < 0.05$ ) (Supplemental Table 4A). Notably, cathelicidin-3 (*CATH3*), cathelicidin-1 (*CATH1*), Avian beta-defensin 1 (*AvBD1*), Avian beta-defensin 7 (*AvBD7*), Interferon induced with helicase C domain 1 (*IFIH1*), RNA binding motif protein 11 (*RBM11*), Mitochondrial rRNA methyltransferase 2 (*MRM2*) were significantly enriched in immune-related terms such as defense response to gram-negative bacteria, positive regulation of interleukin-6 production, innate immune response, macrophage activation, and epigenetic modification-related pathways, including RNA methylation and regulation of alternative mRNA splicing via spliceosome, RNA methyltransferase activity ( $P < 0.05$ ) (Fig. 2C). For KEGG analysis, there were 21 pathways significantly enriched, such as PPAR signaling pathway, steroid hormone biosynthesis, viral protein interaction with cytokine and cytokine receptor, metabolism of xenobiotics by cytochrome P450, and drug metabolism - cytochrome P450 ( $P < 0.05$ ) (Fig. 2D, detailed in Supplemental Table 2B). C-X-C motif chemokine ligand 13-like 2 (*CXCL13L2*) was involved in viral protein interactions with cytokines and cytokine receptors.

#### The variation of alternative splicing following *C. jejuni* inoculation

We characterized the alternative splicing (AS) types in each group and counted the number of significantly different AS types corresponding transcripts in each type. The number of skipping exon (SE) splicing events was the largest (28.2%) of all the AS types, whereas that of the mutually exclusive exons (MX) splicing events was the least (2.02%) (Fig. 3B). We identified 414 significantly different AS events between groups T and C. The highest number of significantly different AS types between T and C groups was SE ( $n = 54$ ) and the least was AL ( $n = 10$ ) (Fig. 3C). The number of unique AS in T group was lower than that in C group (Fig. 3D). Functional enrichment of these significantly different AS events were enriched in immune-related pathways such as basophil activation involved in immune response, pyroptosis, cellular response to biotic stimulus, positive regulation of inflammatory response to antigenic stimulus, regulation of NIK/NF- $\kappa$ B signaling ( $P < 0.05$ ) (Fig. 3E, detailed in Supplemental Table 5A). KEGG enrichment of these significantly different AS events indicated associations with 11 pathways including the p53 signaling pathway, drug metabolism-cytochrome P450, Lysine biosynthesis, Toll

and Imd signaling pathway, and C-type lectin receptor signaling pathway ( $P < 0.05$ ) (Fig. 3E, detailed in Supplemental Table 5B).

#### Poly(A) tail length variation of transcripts following *C.*

##### *jejuni* inoculation

To determine the potential interaction of other factors with transcript expression, we analyzed the poly(A) tail length and expression of the corresponding transcripts. The average length of the poly(A) tails of the transcripts in T group was 84.21, which was shorter than that in C group (86.81) (Fig. 4A). The length of the poly(A) tails of the transcripts was negatively correlated with their expression ( $R_{(C)} = -0.33$ ,  $R_{(T)} = -0.32$ ,  $P < 0.05$ ) (Fig. 4B). Compared to C group, there were 271 transcripts contained shorter poly(A) tails and 155 transcripts contained longer poly(A) tails in T group (Fig. 4C, detailed in Supplemental Table 6). GO annotation results showed that the transcripts contained significantly different poly(A) tail length were highly enriched in some immune-related functional terms including response to stress, defense response, innate immune response, negative regulation of cytokine production, and epigenetic-related terms including RNA splicing and RNA modification ( $P < 0.05$ ) (Fig. 4D, detailed in Supplemental Table 7). Significantly enriched KEGG pathways ( $P < 0.05$ ) were divided into two groups, (1) Metabolism-related pathways including sulfur relay system, porphyrin metabolism, steroid hormone biosynthesis, ubiquitin-mediated proteolysis, ubiquinone and other terpenoid-quinone biosynthesis, and metabolism of xenobiotics by cytochrome P450, (2) Immune-related pathway including apoptosis - multiple species (Fig. 4E).

#### The profiling of m<sup>5</sup>C modification in the transcripts

We captured the genetic features of the 9 bp m<sup>5</sup>C methylation sites in T and C groups. The positions of the first, second, fourth, and eighth bases in the m<sup>5</sup>C methylation sites were changed between T and C groups (Fig. 5A). Followed by the 3'UTR region, the m<sup>5</sup>C sites in T and C groups were mainly distributed in the CDS region (Fig. 5B). The proportion of m<sup>5</sup>C sites on different chromosomes in T group was similar to that in C group, with the highest proportion on Chr 1 (Fig. 5C). There were 29 DETs containing m<sup>5</sup>C modifications, of which, 14 were upregulated and 15 were downregulated in T group compared with C group (Fig. 5D, detailed in Supplemental Table 8A). These DETs containing m<sup>5</sup>C modifications were significantly enriched in 140 GO terms, including 93 BP, 34 MF, and 13 CC terms ( $P < 0.05$ ) (Supplemental Table 8B). For BP terms, regulation of interferon-alpha production, response to xenobiotic stimulus, immune response-regulating signaling pathway, macrophage activation involved in immune response, toll-like receptor

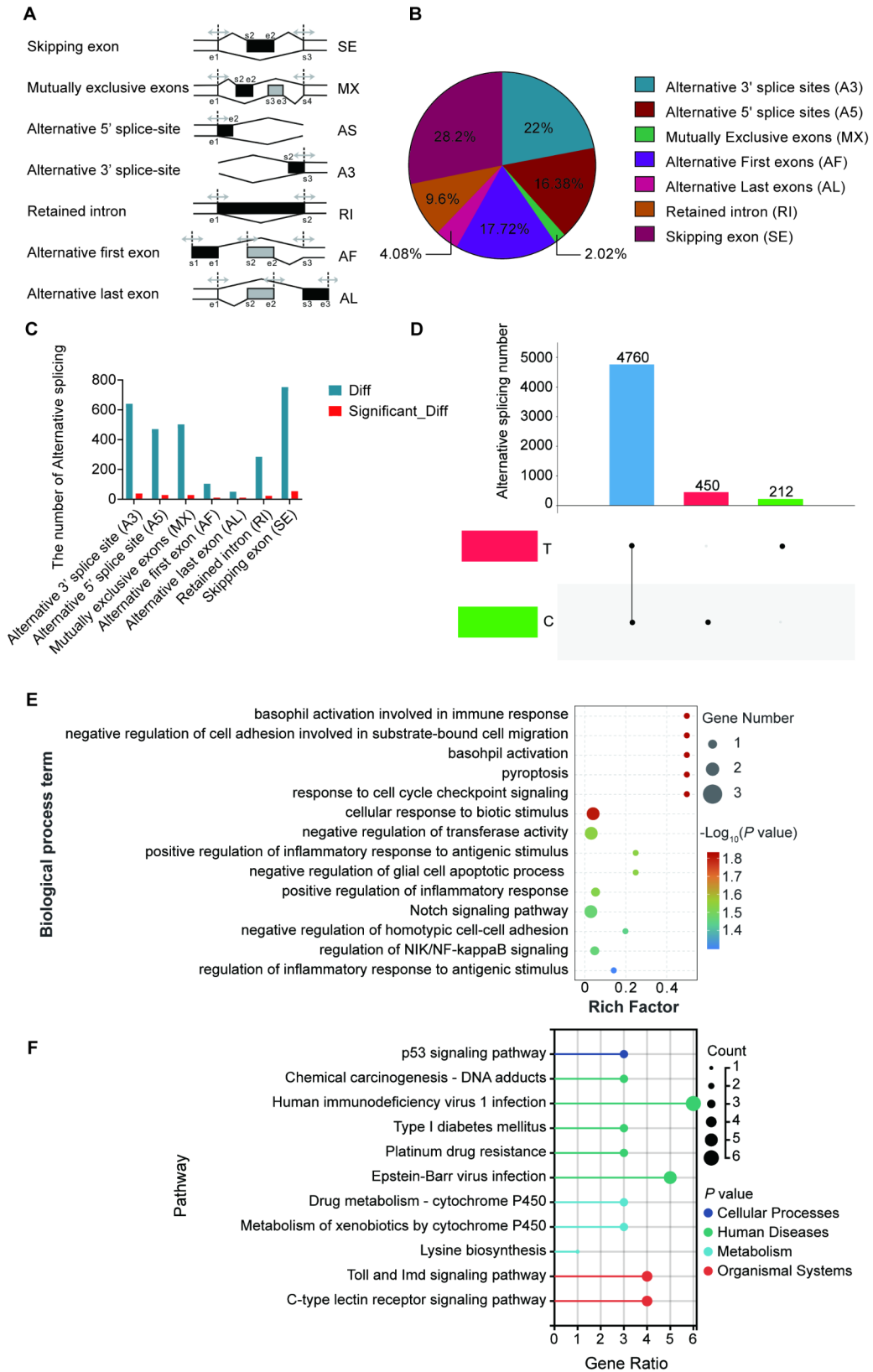


**Fig. 3** The pattern of AS of chicken following *C. jejuni* inoculation. **(A)** The type of AS. **(B)** The proportion of alternative splicing of different types. **(C)** The number of different AS under every type between C group and T. **(D)** The total number of unique AS. **(E)** GO analysis of significantly different AS events. **(F)** KEGG pathway of significantly different AS events

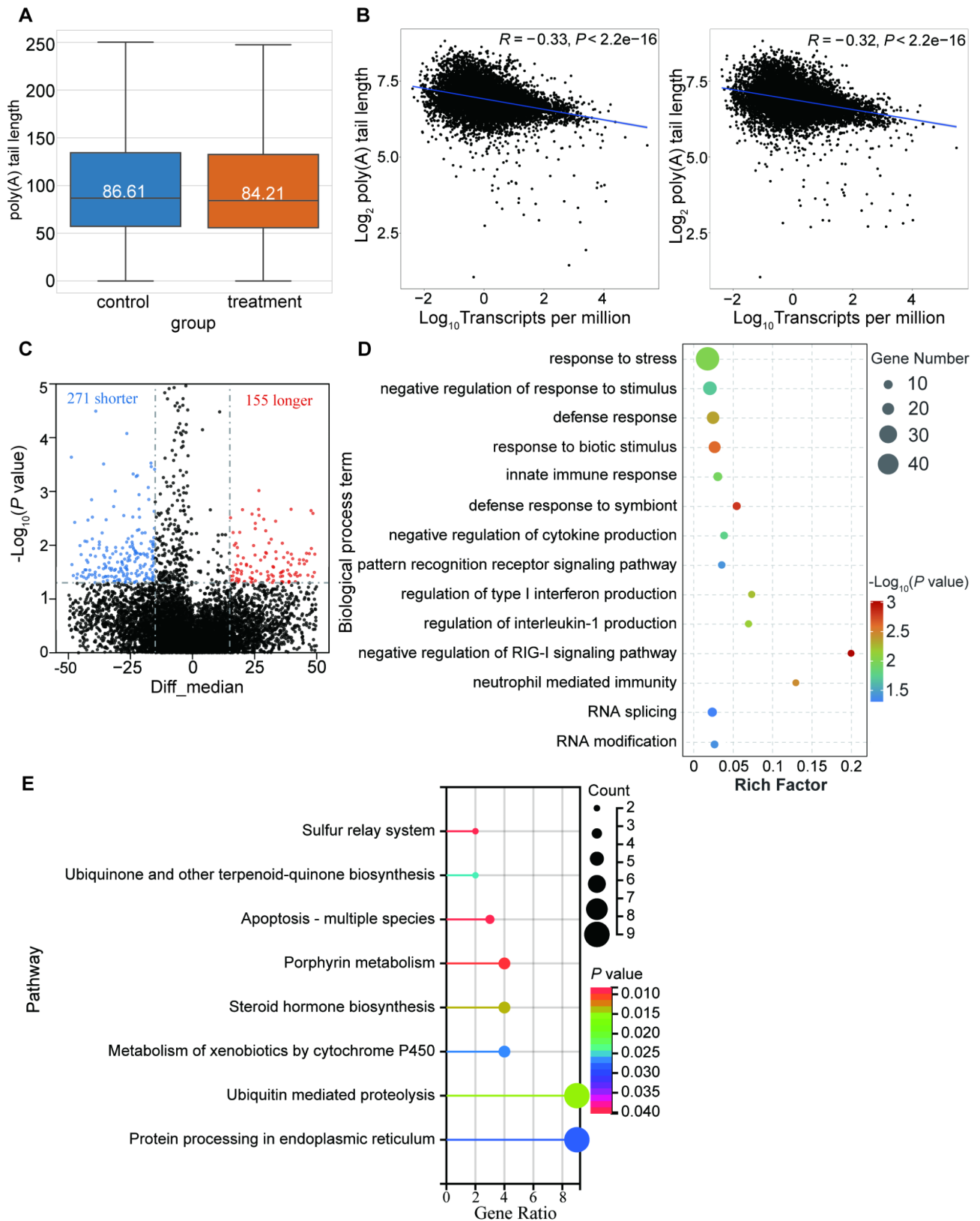


**Fig. 4** Poly(A) tail length variation of transcripts following *C. jejuni* inoculation. **(A)** The mean length of the poly(A) tails on the transcripts. **(B)** Pearson correlation analysis between poly(A) tail length and expression level of transcripts of C (right) and T groups (left). **(C)** Volcano plot of different length of the poly(A) tails between C and T groups. **(D)** GO analysis of significantly different length of the poly(A) tails. **(E)** KEGG pathway of significantly different length of the poly(A) tails

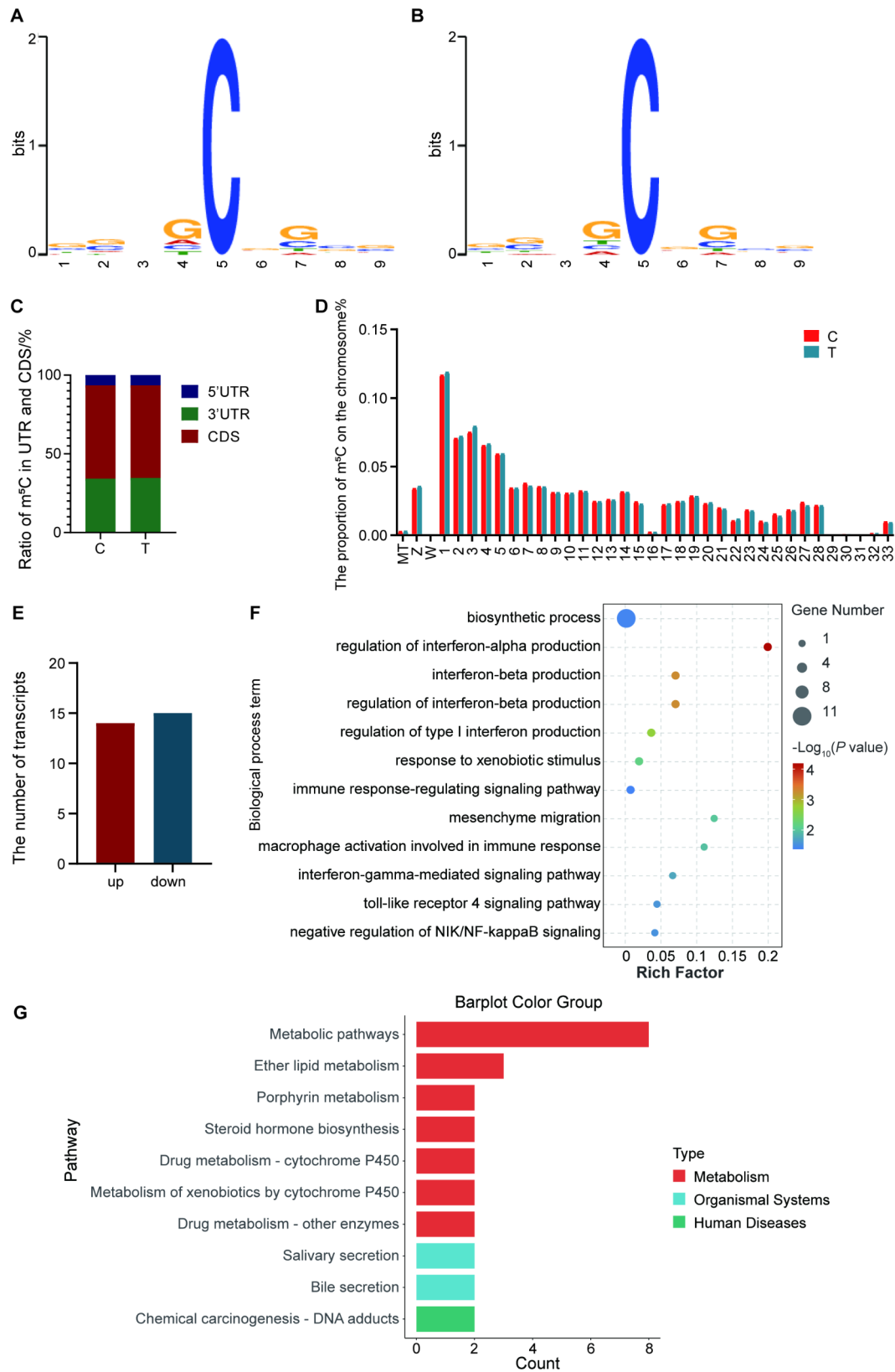


**Fig. 5** Profiling of m<sup>5</sup>C modification in the transcripts following *C. jejuni* inoculation. **(A)** The genetic features of the 9 bp long m<sup>5</sup>C methylation sites of C (right) and T (left) groups. **(B)** The ratio of m<sup>5</sup>C-modified sites distributed in the 5'UTR, CDS, and 3'UTR of C and T groups. **(C)** The proportion of m<sup>5</sup>C sites on the chromosome in C and T groups. **(D)** The number of differentially expressed transcripts containing m<sup>5</sup>C sites. **(E)** GO analysis of differentially expressed transcripts containing m<sup>5</sup>C sites. **(F)** KEGG pathway of differentially expressed transcripts containing m<sup>5</sup>C sites

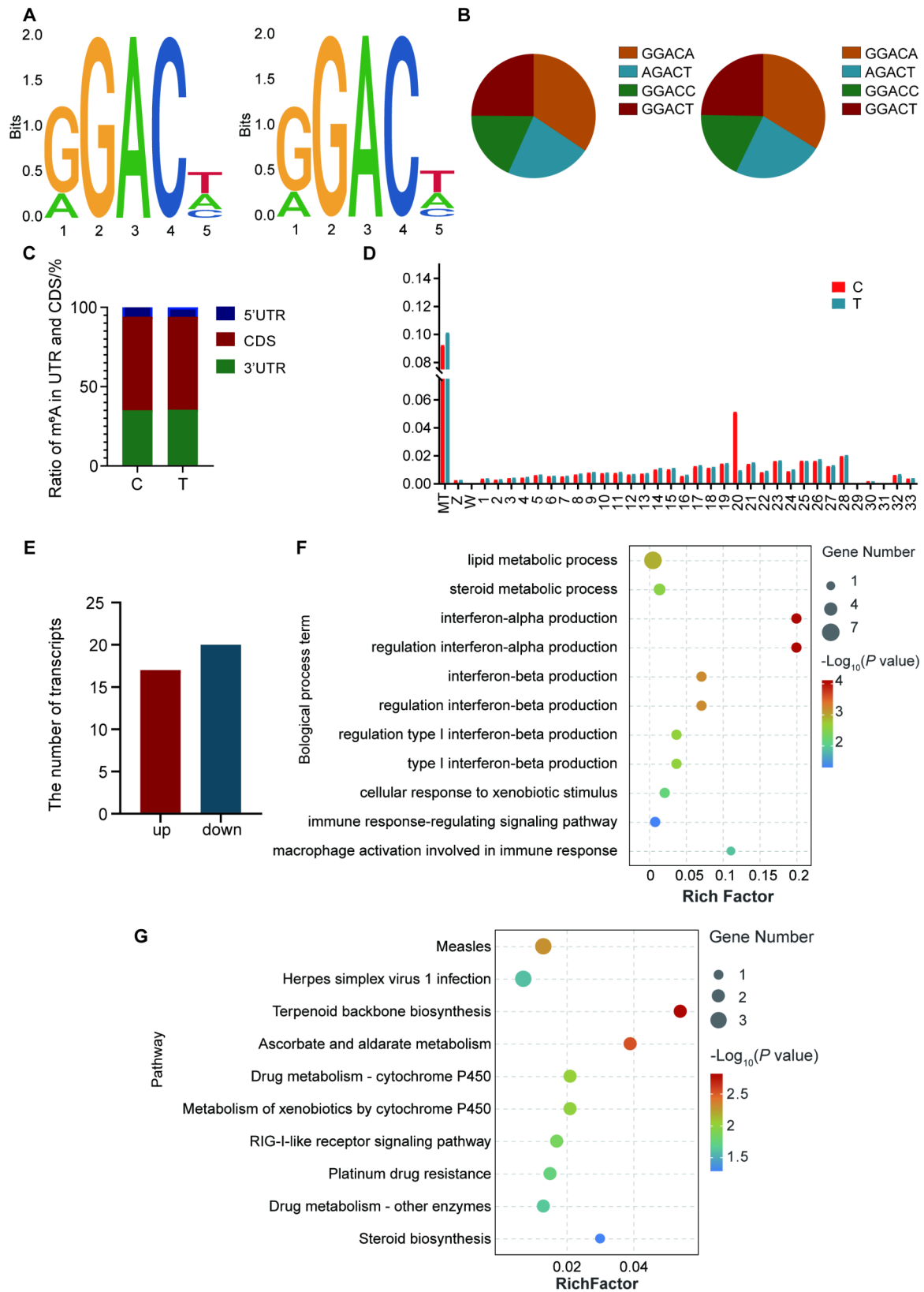


**Fig. 6** (See legend on next page.)

(See figure on previous page.)

**Fig. 6** Profiling of m<sup>6</sup>A modification in the transcripts following *C. jejuni* inoculation. **(A)** The genetic features of the 5 bp long m<sup>6</sup>A methylation sites of C (right) and T (left) groups. **(B)** The proportion of m<sup>6</sup>A motif of C (right) and T (left) groups. **(C)** The ratio of m<sup>6</sup>A-modified sites distributed in the 5'UTR, CDS, and 3'UTR of C and T groups. **(D)** The proportion of m<sup>6</sup>A sites on the chromosome in C and T groups. **(E)** The number of differentially expressed transcripts containing m<sup>6</sup>A sites. **(F)** GO analysis of differentially expressed transcripts containing m<sup>6</sup>A sites. **(G)** KEGG pathway of differentially expressed transcripts containing m<sup>6</sup>A sites

4 signaling pathway, and negative regulation of NIK/NF- $\kappa$ B signaling were significantly enriched (Fig. 5E). KEGG analysis results showed that these DETs containing m<sup>5</sup>C modifications were significantly enriched in 18 pathways ( $P < 0.05$ ) (Supplemental Table 8C) including ether lipid metabolism, steroid hormone biosynthesis, drug metabolism - cytochrome P450, bile secretion, drug metabolism - other enzymes (Fig. 5F).

### The profiling of m<sup>6</sup>A modification in the transcripts

The features of 5 bp m<sup>6</sup>A methylation sites in T and C groups were similar (Fig. 6A). The proportion of GGACA motif was the highest among all m<sup>6</sup>A motifs, representing 33.8% and 33.4% in T and C groups, respectively. The GGACC motif was the least abundant motif, representing approximately 18.1% and 18.4% in T and C groups, respectively (Fig. 6B). Similar to the m<sup>5</sup>C modification, the m<sup>6</sup>A sites in T and C groups were mainly located in the CDS region (Fig. 6C). Except for chromosome 20, the m<sup>6</sup>A density on different chromosomes in T group was higher than that in C group (Fig. 6D). The global level of m<sup>6</sup>A decreased substantially following *C. jejuni* inoculation (Supplemental Fig. 1). There were 37 DETs containing m<sup>6</sup>A modifications, with 17 upregulated and 20 downregulated transcripts in T group compared with C group (Fig. 6E, detailed in Supplemental Table 9A). Those DETs were significantly enriched in 148 GO terms (96 BP, 46 ME, and 6 CC) ( $P < 0.05$ ) (Supplemental Table 9B). Enriched BP terms mainly focused on the regulation of interferon-alpha production, interferon-beta production, cellular response to xenobiotic stimulus, type I interferon production, immune response regulating signaling pathway, and macrophage activation involved in the immune response (Fig. 6F). Twenty KEGG pathways were significantly enriched ( $P < 0.05$ ), such as RIG-I-like receptor signaling pathway, platinum drug resistance, drug metabolism - other enzymes, steroid biosynthesis (Fig. 6G, detailed in Supplemental Table 9C).

### Joint analysis of post-transcriptional modification following *C. jejuni* inoculation

To further clarify the function of m<sup>5</sup>C and m<sup>6</sup>A, we analyzed the correlation between m<sup>5</sup>C/m<sup>6</sup>A modifications and the expression of their target transcripts. The expression of transcripts containing m<sup>5</sup>C or m<sup>6</sup>A was significantly higher than that of the transcripts with no modification ( $P < 0.05$ ). M<sup>5</sup>C- modified transcripts with higher fractions had higher expression levels, whereas

m<sup>6</sup>A- modified transcripts with lower fractions had higher expression levels ( $P < 0.05$ ) (Fig. 7A and B). To discover the interaction between m<sup>5</sup>C and m<sup>6</sup>A, we compared the expression of transcripts with both modifications to that of transcripts with one modification. Transcripts containing both modifications had relatively higher expression levels than those with only m<sup>6</sup>A modifications or without modifications (Fig. 7C). In contrast to m<sup>6</sup>A, transcripts with only m<sup>5</sup>C modifications showed relatively higher expression levels than those with both modifications or without modifications (Fig. 7D). m<sup>5</sup>C- or m<sup>6</sup>A- modified transcripts had significantly shorter poly(A) tail lengths than those without modifications (Fig. 7E). Intriguingly, only m<sup>5</sup>C- modified transcripts had the shortest poly(A) tail length compared to those only m<sup>6</sup>A- modified transcripts and without modifications (Fig. 7F). These results indicated that m<sup>5</sup>C was more effective in promoting the expression of transcripts. Additionally, their impact on poly(A) tail length was opposite to that on the expression.

To further verify the crucial process and hub genes of chicken responding to *C. jejuni* inoculation, we merged GO terms of these modules, including DETs, transcripts with differentially significant poly(A) tail length, m<sup>5</sup>C modified DETs, and m<sup>6</sup>A modified DETs. Terms like response to the virus and negative regulation of interferon-beta production were identified ( $P < 0.05$ ) (Fig. 7G). Specially, ENSGALT00000020390 (novel transcript), and ENSGALT00000053962 (IFIH1-202) were significantly enriched ( $P < 0.05$ ). Furthermore, we visualized the m<sup>6</sup>A/m<sup>5</sup>C modifications on these two target genes between C and T groups. Compared to C group, T group had more m<sup>6</sup>A and m<sup>5</sup>C sites on these two target transcripts, novel transcript ENSGALT00000020390 only had m<sup>6</sup>A sites without m<sup>5</sup>C site (Fig. 7G, detailed in the Supplemental Fig. 2).

### Discussion

As an enteric pathogen in the chicken gut, *C. jejuni* significantly impacts gut permeability and organ invasion, posing a tremendous threat to poultry health [38]. RNA post-transcriptional modifications (PTMs) are a pervasive features common to all domains of organisms [39]. Accumulating evidence shows that PTMs can influence the fundamental characteristics and functions of RNAs, including their structure, stability, cellular localization and inter-molecular interactions [40, 41].

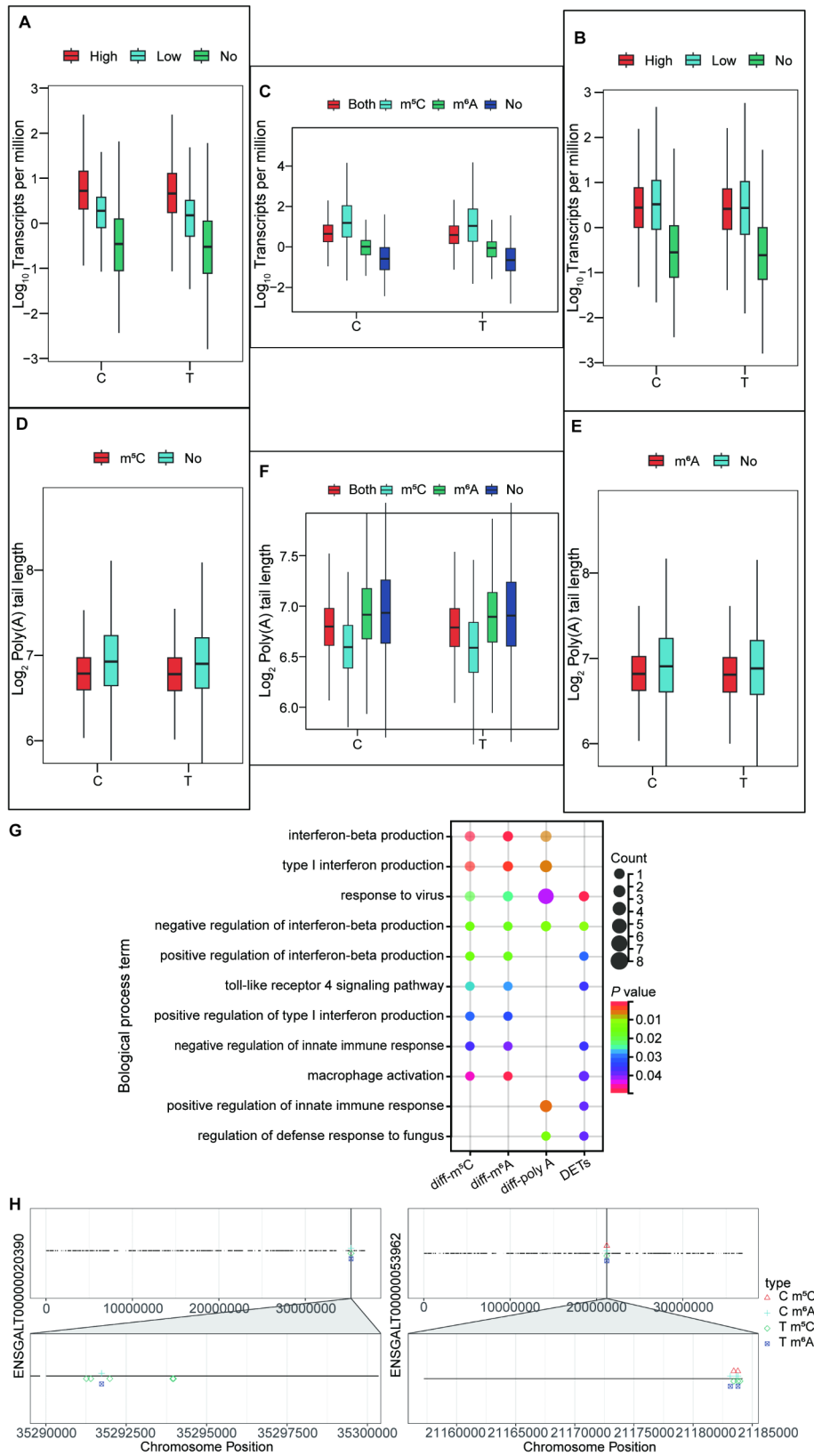


**Fig. 7** (See legend on next page.)

(See figure on previous page.)

**Fig. 7** Conjoint analysis of epigenetic modifications following *C. jejuni* inoculation. **(A)** Comparison of the expression level of transcripts with and without m<sup>5</sup>C modification in C and T groups. High indicates the transcripts with the maximum fraction ranging from 0.9 to 1.0; low indicates the transcripts with the maximum fraction ranging from 0.7 to 0.9; no indicates the transcripts without m<sup>5</sup>C modification. **(B)** Comparison of the expression level of transcripts with and without m<sup>6</sup>A modification in C and T groups. High indicates the transcripts with the maximum fraction ranging from 0.5 to 1.0; low indicates the transcripts with the maximum fraction ranging from 0.0 to 0.5; no indicates the transcripts without m<sup>6</sup>A modification. **(C)** The expression level of transcripts with different modifications. Both indicates the transcripts modified by both m<sup>6</sup>A and m<sup>5</sup>C; m<sup>6</sup>A indicates the transcripts modified by m<sup>6</sup>A only; m<sup>5</sup>C indicates the transcripts modified by m<sup>5</sup>C only; no indicates the transcripts without m<sup>6</sup>A and m<sup>5</sup>C modifications. **(D)** Comparison of poly(A) tail length of transcripts with and without m<sup>6</sup>A modification in C and T groups. m<sup>6</sup>A indicates the transcripts modified by m<sup>6</sup>A; no indicates the transcripts not modified by m<sup>6</sup>A. **(E)** Comparison of poly(A) tail length of transcripts with and without m<sup>5</sup>C modification in C and T groups. m<sup>5</sup>C indicates the transcripts modified by m<sup>5</sup>C; no indicates the transcripts not modified by m<sup>5</sup>C. **(F)** The poly(A) tail length of transcripts with different modifications. **(G)** The intersection of GO terms of the DETs, differential poly(A) tail length corresponding to transcripts, m<sup>5</sup>C modified DETs, and m<sup>6</sup>A modified DETs modules. **(H)** The chromosomal location of m<sup>5</sup>C and m<sup>6</sup>A of ENSGALT00000020390 (novel transcript) (left) and ENSGALT00000053962 (*IFH1*) (right) in C and T groups. m<sup>6</sup>A: depth > 10, fraction > 0.5; m<sup>5</sup>C: depth > 10, fraction > 0.7

In this study, we determined an unbiased quantitative transcriptome and profiled post-transcriptional modifications with manifestation in novel transcripts, alternative splicing, poly(A) tails, m<sup>5</sup>C methylation, and m<sup>6</sup>A methylation of chicken cecum following *C. jejuni* inoculation by direct RNA sequencing, providing a more authentic and comprehensive snapshot of the RNA landscape in the response to *C. jejuni* inoculation. We identified 8,560 novel genes and 10,503 novel transcripts. GO enrichment and KEGG analysis result showed that these novel transcripts were mainly associated with immune related processes like apoptotic process, NOD-like receptor signaling pathway, chemokine signaling pathway, Wnt signaling pathway, Ras signaling pathway, and mTOR signaling pathway. These pathways have been proved to be associated with the immune response to bacterial infections [42, 43]. Our results suggest that the response of chicken to *C. jejuni* inoculation mainly involved in the above aspects of immune-related biological processes, and further improving the annotation of the chicken genome responding to *C. jejuni* inoculation and obtaining new information on their functions.

Notably, we also performed alternative splicing analysis, and most of the specific alternative splicing events of T group were fewer than those of C group. Alternative splicing events is universal phenomenon in functionally coordinated and biologically important networks in the context of physiologically normal and disease status [44]. Transcripts usually undergo one or more forms of alternative splicing [45]. In our study, these specific alternative splicing events corresponding to transcripts were mainly enriched in immune-related terms such as basophil activation involved in immune response, pyroptosis, cellular response to biotic stimulus, positive regulation of inflammatory response to antigenic stimulus, Notch signaling pathway, and regulation of NIK/NF- $\kappa$ B signaling. Aberrant RNA splicing can produce the abnormal modulation of immune activity in infections and immune diseases [46]. Co-incubation of HeLa cells with *C. jejuni* triggers the activation of the transcription factor NF- $\kappa$ B [47]. It was speculated that *C. jejuni* inoculation could inhibit the production of alternative splicing and thus regulate

the immune response process. Poly(A) tails are bound by the cytoplasmic polyadenylate-binding protein (PABPC), thus promote translation and prevent mRNA degradation [7]. Here, the length of the poly(A) tails of the transcripts was negatively correlated with their expression levels. The length of poly(A) tail might be coupled to the gene expression level, the transcripts with high expression level contain relatively short tails [48].

m<sup>6</sup>A is increasingly recognized as an important modification for the regulation of different RNAs in physiological and pathological contexts [49, 50]. In the present study, the global m<sup>6</sup>A levels were suppressed following *C. jejuni* inoculation, indicating that m<sup>6</sup>A modification may be involved in the regulation of *C. jejuni* inoculation. We further quantified the distribution and density of m<sup>6</sup>A sites. Most m<sup>6</sup>A sites were distributed in the CDS region of mRNA, which is consistent with previous studies [51, 52]. Intriguingly, the position of the m<sup>6</sup>A sites did not change following *C. jejuni* inoculation while the position of the forth base in the m<sup>5</sup>C methylation site changed. Zhou et al. [53] found that the position of the second base in the m<sup>5</sup>C methylation site changed during sex differentiation, while the m<sup>6</sup>A sequence features did not change. We suspect that changes in the m<sup>5</sup>C methylation site may occur during some biological processes. Notably, these transcripts are mainly involved in the immune-related process such as defense response to gram-negative bacterium, CCR6 chemokine receptor binding, cytolysis, and innate immune response, which have all been reported in previous studies [54–57]. Additionally, the terms like RNA methyltransferase activity was enriched, further supporting our hypothesis that m<sup>6</sup>A modification may be involved in the regulation of *C. jejuni* inoculation. The biological importance of m<sup>6</sup>A and m<sup>5</sup>C has been previously confirmed [58, 59].

We clarified the relationship between m<sup>6</sup>A/m<sup>5</sup>C modification and the expression level of their targeted transcripts, and found that transcripts containing m<sup>6</sup>A/m<sup>5</sup>C modification displayed higher expression levels and shorter poly(A) tails than those without modification, which is consistent with previous research [60]. Particularly, no interactions were observed between m<sup>6</sup>A

and m<sup>5</sup>C. These modifications can affect the stability or translation efficiency of the target mRNAs [61]. To determine the crucial process and hub genes response to *C. jejuni* inoculation, we performed a joint analysis of the intersection of GO terms of these modules including the DETs, differential poly(A) tail length corresponding to transcripts, m<sup>5</sup>C modified DETs, and m<sup>6</sup>A modified DETs. ENSGALT00000020390 (novel transcript), and ENSGALT00000053962 (IFIH1-202) were significantly enriched. *IFIH1* gain-of-function has been reported as a cause of a type I interferon pathology encompassing a spectrum of auto inflammatory phenotypes [62]. *IFIH1* as an innate immune receptor plays a major role in sensing viral infection and in the activation of a cascade of antiviral responses including the induction of type I interferons and pro-inflammatory cytokines [63]. These studies further support ENSGALG00000012480 (novel gene), and *IFIH1* could be potential candidate genes following *C. jejuni* inoculation. Furthermore, we visualized the m<sup>6</sup>A/m<sup>5</sup>C modifications on these two target genes between C and T groups to better clarify the detailed position of methylation modifications. Compared to C group, T group had more m<sup>6</sup>A and m<sup>5</sup>C sites on these two target transcripts, indicating that methylation modifications were more likely to occur following *C. jejuni* inoculation.

## Conclusions

In conclusion, post-transcriptional modifications, including alternative splicing, poly(A) tails and methylation modifications are associated with the immune defense process against *C. jejuni* inoculation. *C. jejuni* inoculation mainly involved in immune-related biological processes such as defense response to gram-negative bacterium, CCR6 chemokine receptor binding, mTOR signaling pathway and negative regulation of interferon-beta production. ENSGALG00000012480 (novel gene), and *IFIH1* could be potential candidate genes following *C. jejuni* inoculation. The findings herein will contribute to a better understanding of the immune mechanisms of chickens following *C. jejuni* inoculation. However, further studies are still needed to provide the detailed evidence for the response to *C. jejuni* inoculation.

## Supplementary Information

The online version contains supplementary material available at <https://doi.org/10.1186/s12864-025-11564-3>.

Supplemental Table 1. The quality control and alignment of sequencing data. (A) The quality control of sequencing data. (B) Reads alignment of sequencing data

Supplemental Table 2. The detailed primers for mRNAs

Supplemental Table 3. The significantly enriched GO terms and KEGG pathways of novel transcripts. (A) The significantly enriched GO terms of novel transcripts ( $P < 0.05$ ). (B) The enriched KEGG pathways of novel transcripts ( $P < 0.05$ )

Supplemental Table 4. The significantly enriched GO terms and KEGG pathways of DETs. (A) The significantly enriched GO terms of DETs ( $P < 0.05$ ). (B) The significantly enriched KEGG pathways of DETs ( $P < 0.05$ )

Supplemental Table 5. The significantly enriched GO terms and KEGG pathways of differential alternative splicing corresponding to transcripts. (A) The significantly enriched GO terms of differential alternative splicing corresponding to transcripts ( $P < 0.05$ ). (B) The significantly enriched KEGG pathways of differential alternative splicing corresponding to transcripts ( $P < 0.05$ )

Supplemental Table 6. The concrete transcripts containing the different length of the poly(A) tails ( $P < 0.05$ )

Supplemental Table 7. The significantly enriched GO terms of different poly(A) tail length corresponding to transcripts ( $P < 0.05$ )

Supplemental Table 8. The function of DETs containing m<sup>5</sup>C site. (A) DETs containing m<sup>5</sup>C site ( $P < 0.05$ ). (B) The significantly enriched GO terms of DETs containing m<sup>5</sup>C site ( $P < 0.05$ ). (C) The significantly enriched KEGG pathways of DETs containing m<sup>5</sup>C site ( $P < 0.05$ )

Supplemental Fig. 1. Supplemental analysis of m<sup>6</sup>A modification. (A) The qRT-PCR analysis of *METTL3/METTL14* expression level in cecum of groups C and T. (B) The global level of m<sup>6</sup>A in cecum of groups C and T by Dot blot

Supplemental Table 9. The function of DETs containing m<sup>6</sup>A site. (A) DETs containing m<sup>6</sup>A site ( $P < 0.05$ ). (B) The significantly enriched GO terms of DETs containing m<sup>6</sup>A site ( $P < 0.05$ ). (C) The significantly enriched KEGG pathways of DETs containing m<sup>6</sup>A site ( $P < 0.05$ )

Supplemental Fig. 2. The IGV analysis of m<sup>6</sup>A/m<sup>5</sup>C methylation modifications on ENSGALT00000020390 (novel transcript), and ENSGALT00000053962 (IFIH1-202). (A) The m<sup>6</sup>A methylation modifications on ENSGALT00000020390 (novel transcript) of groups C and T. The abscissa represents the position of the chromosome, and the ordinate represents the fraction on the location site. Filtering: depth > 10, fraction > 0. (B) The m<sup>6</sup>A methylation modifications on ENSGALT00000053962 (IFIH1-202). The abscissa represents the position of the chromosome, and the ordinate represents the fraction on the location site. Filtering: depth > 10, fraction > 0. (C) The m<sup>5</sup>C methylation modifications on ENSGALT00000053962 (IFIH1-202). The abscissa represents the position of the chromosome, and the ordinate represents the fraction on the location site. Filtering: depth > 10, fraction > 0.5

## Acknowledgements

Not applicable.

## Author contributions

Y.-N.Z.: Software, Methodology, Data curation, Writing—original draft, Writing—review & editing. Y.-M.W.: Data curation, Methodology, Writing—review & editing. Y.-R.R.: Data curation, Methodology, Writing—review & editing. L.L.: Data curation, Writing—review & editing. T.-Y.W.: Data curation, Writing—review & editing. L.-Y.L.: Investigation, Writing—review & editing. X.-Y.L.: Conceptualization, Funding acquisition, Supervision, Writing—review & editing. All authors reviewed the manuscript.

## Funding

This work was supported by National Key Research and Development Program of China (2022YFD1300102, 2021YFD1300102), Key R&D Program of Shandong Province, China (2023LZGC018, 2022LZGC013), Shandong Modern Agricultural Industry and Technology System (SDAIT-11-02).

## Data availability

The raw data generated in the current study have been deposited to the National Genomics Data Center (NGDC; <https://ngdc.cncb.ac.cn>) with accession number PRJCA012851. <https://submission.springernature.com/new/submission/008d1420-5421-4859-ae44-743e09e1aedf/review>.

## Declarations

### Ethics approval and consent to participate

The present study protocol was approved by the Ethics Committee on the Care and Use of Laboratory Animals at Shandong Agricultural University (Tai'an, China) (Number: SDAUA-2019-060). The Guiding Principles for the Care and Use of Research Animals and Animal Research: Reporting In Vivo Experiments (ARRIVE guidelines) were followed in all animal experimentation methods. All methods and procedures described in this paper were carried out in accordance with European Union Directive 2010/63/EU.

### Consent for publication

Not applicable.

### Competing interests

The authors declare no competing interests.

Received: 22 November 2024 / Accepted: 2 April 2025

Published online: 14 April 2025

## References

- Greige S, Rivoal K, Osman M, Safadi DE, Dabboussi F, Hage RE, Viscogliosi E, Hamze M, Chemaly M. Prevalence and genetic diversity of *Campylobacter* Spp. In the production chain of broiler chickens in Lebanon and its association with the Intestinal protozoan *blastocystis* Sp. *Poult Sci*. 2019;98(11):5883–91.
- Kemper L, Hensel A. *Campylobacter* Jejuni: targeting host cells, adhesion, invasion, and survival. *Appl Microbiol Biotechnol*. 2023;107(9):2725–54.
- Ijaz UZ, Sivaloganathan L, McKenna A, Richmond A, Kelly C, Linton M, Stratakos AC, Lavery U, Elmi A, Wren BW, et al. Comprehensive longitudinal Microbiome analysis of the chicken cecum reveals a shift from competitive to environmental drivers and a window of opportunity for *Campylobacter*. *Front Microbiol*. 2018;9:2452.
- Allen VM, Bull SA, Corry JE, Domingue G, Jørgensen F, Frost JA, Whyte R, Gonzalez A, Elviss N, Humphrey TJ. *Campylobacter* spp. Contamination of chicken carcasses during processing in relation to flock colonisation. *Int J Food Microbiol*. 2007;113(1):54–61.
- Wagle BR, Donoghue AM, Shrestha S, Upadhyaya I, Arsi K, Gupta A, Liyanage R, Rath NC, Donoghue DJ, Upadhyay A. Carvacrol attenuates *Campylobacter* jejuni colonization factors and proteome critical for persistence in the chicken gut. *Poult Sci*. 2020;99(9):4566–77.
- Sun H, Li K, Liu C, Yi C. Regulation and functions of non-m(6)A mRNA modifications. *Nat Rev Mol Cell Biol*. 2023;24(10):714–31.
- Passmore LA, Collier J. Roles of mRNA poly(A) Tails in regulation of eukaryotic gene expression. *Nat Rev Mol Cell Biol*. 2022;23(2):93–106.
- Kwak Y, Daly CWP, Fogarty EA, Grimson A, Kwak H. Dynamic and wide-spread control of poly(A) tail length during macrophage activation. *RNA*. 2022;28(7):947–71.
- Banerjee S, Galarza-Muñoz G, Garcia-Blanco MA. Role of RNA alternative splicing in T cell function and disease. *Genes (Basel)* 2023, 14(10).
- Kjer-Hansen P, Weatheritt RJ. The function of alternative splicing in the proteome: rewiring protein interactomes to put old functions into new contexts. *Nat Struct Mol Biol*. 2023;30(12):1844–56.
- Zou C, Zan X, Jia Z, Zheng L, Gu Y, Liu F, Han Y, Xu C, Wu A, Zhi Q. Crosstalk between alternative splicing and inflammatory bowel disease: basic mechanisms, biotechnological progresses and future perspectives. *Clin Transl Med*. 2023;13(11):e1479.
- Dery KJ, Kojima H, Kageyama S, Kadono K, Hirao H, Cheng B, Zhai Y, Farmer DG, Kaldas FM, Yuan X, et al. Alternative splicing of CEACAM1 by hypoxia-inducible factor-1 $\alpha$  enhances tolerance to hepatic ischemia in mice and humans. *Sci Transl Med*. 2023;15(707):eadf2059.
- Wojtyś W, Orofi M. How driver oncogenes shape and are shaped by alternative splicing mechanisms in tumors. *Cancers (Basel)* 2023, 15(11).
- Molinie B, Wang J, Lim KS, Hillebrand R, Lu ZX, Van Wittenbergh N, Howard BD, Daneshvar K, Mullen AC, Dedon P, et al. m(6)A-LAIC-seq reveals the census and complexity of the m(6)A epitranscriptome. *Nat Methods*. 2016;13(8):692–8.
- Zhou J, Wan J, Gao X, Zhang X, Jaffrey SR, Qian SB. Dynamic m(6)A mRNA methylation directs translational control of heat shock response. *Nature*. 2015;526(7574):591–4.
- Edupaganti RR, Geiger S, Lindeboom RGH, Shi H, Hsu PJ, Lu Z, Wang SY, Baltissen MPA, Jansen P, Rossa M, et al. N(6)-methyladenosine (m(6)A) recruits and repels proteins to regulate mRNA homeostasis. *Nat Struct Mol Biol*. 2017;24(10):870–8.
- Li M, Tao Z, Zhao Y, Li L, Zheng J, Li Z, Chen X. 5-methylcytosine RNA methyltransferases and their potential roles in cancer. *J Transl Med*. 2022;20(1):214.
- Chen B, Hong Y, Zhai X, Deng Y, Hu H, Tian S, Zhang Y, Ren X, Zhao J, Jiang C. m6A and m5C modification of GPX4 facilitates anticancer immunity via STING activation. *Cell Death Dis*. 2023;14(12):809.
- Batista PJ, Molinie B, Wang J, Qu K, Zhang J, Li L, Bouley DM, Lujan E, Haddad B, Daneshvar K, et al. m(6)A RNA modification controls cell fate transition in mammalian embryonic stem cells. *Cell Stem Cell*. 2014;15(6):707–19.
- Li HB, Tong J, Zhu S, Batista PJ, Duffy EE, Zhao J, Bailis W, Cao G, Kroehling L, Chen Y, et al. m(6)A mRNA methylation controls T cell homeostasis by targeting the IL-7/STAT5/SOCS pathways. *Nature*. 2017;548(7667):338–42.
- Sun G, Ma S, Zheng Z, Wang X, Chen S, Chang T, Liang Z, Jiang Y, Xu S, Liu R. Multi-omics analysis of expression and prognostic value of NSUN members in prostate cancer. *Front Oncol*. 2022;12:965571.
- Yu G, Bao J, Zhan M, Wang J, Li X, Gu X, Song S, Yang Q, Liu Y, Wang Z, Xu B. Comprehensive analysis of m5C methylation regulatory genes and tumor microenvironment in prostate cancer. *Front Immunol*. 2022;13:914577.
- Song D, An K, Zhai W, Feng L, Xu Y, Sun R, Wang Y, Yang YG, Kan Q, Tian X. NSUN2-mediated mRNA m(5)C modification regulates the progression of hepatocellular carcinoma. *Genomics Proteom Bioinf*. 2023;21(4):823–33.
- Humphrey S, Chaloner G, Kemmett K, Davidson N, Williams N, Kipar A, Humphrey T, Wigley P. *Campylobacter jejuni* is not merely a commensal in commercial broiler chickens and affects bird welfare. *mBio*. 2014;5(4):e01364–01314.
- Zheng HX, Zhang XS, Sui N. Advances in the profiling of N(6)-methyladenosine (m(6)A) modifications. *Biotechnol Adv*. 2020;45:107656.
- De Coster W, D'Hert S, Schultz DT, Cruets M, Van Broeckhoven C. NanoPack: visualizing and processing long-read sequencing data. *Bioinformatics*. 2018;34(15):2666–9.
- Wang JR, Holt J, McMillan L, Jones CD. FMLRC: hybrid long read error correction using an FM-index. *BMC Bioinformatics*. 2018;19(1):50.
- Li H. Minimap2: pairwise alignment for nucleotide sequences. *Bioinformatics*. 2018;34(18):3094–100.
- Tang AD, Soulette CM, van Baren MJ, Hart K, Hrabeta-Robinson E, Wu CJ, Brooks AN. Full-length transcript characterization of SF3B1 mutation in chronic lymphocytic leukemia reveals downregulation of retained introns. *Nat Commun*. 2020;11(1):1438.
- Pertea M, Pertea GM, Antonescu CM, Chang TC, Mendell JT, Salzberg SL. StringTie enables improved reconstruction of a transcriptome from RNA-seq reads. *Nat Biotechnol*. 2015;33(3):290–5.
- Pertea G, Pertea M. GFF Utilities: GffRead and GffCompare. *F1000Res* 2020, 9.
- Patro R, Duggal G, Love MI, Irizarry RA, Kingsford C. Salmon provides fast and bias-aware quantification of transcript expression. *Nat Methods*. 2017;14(4):417–9.
- Trincado JL, Entizne JC, Hysenaj G, Singh B, Skalic M, Elliott DJ, Eyraas E. SUPPA2: fast, accurate, and uncertainty-aware differential splicing analysis across multiple conditions. *Genome Biol*. 2018;19(1):40.
- Stoiber M, Quick J, Egan R, Eun Lee J, Celniker S, Neely RK, Loman N, Pennacchio LA, Brown J. *De novo Identification of DNA Modifications Enabled by Genome-Guided Nanopore Signal Processing*. *bioRxiv* 2017:094672.
- Bailey TL, Boden M, Buske FA, Frith M, Grant CE, Clementi L, Ren J, Li WW, Noble WS. MEME SUITE: tools for motif discovery and searching. *Nucleic Acids Res* 2009, 37(Web Server issue):W202–208.
- Akalin A, Kormaksson M, Li S, Garrett-Bakelman FE, Figueroa ME, Melnick A, Mason CE. MethylKit: a comprehensive R package for the analysis of genome-wide DNA methylation profiles. *Genome Biol*. 2012;13(10):R87.
- Wu T, Hu E, Xu S, Chen M, Guo P, Dai Z, Feng T, Zhou L, Tang W, Zhan L, et al. ClusterProfiler 4.0: A universal enrichment tool for interpreting omics data. *Innov (Camb)*. 2021;2(3):100141.
- Al Hakeem WG, Acevedo Villanueva KY, Selvaraj RK. The development of gut microbiota and its changes following *C. jejuni* infection in broilers. *Vaccines (Basel)* 2023, 11(3).
- Leger A, Amaral PP, Pandolfini L, Capitanich C, Capraro F, Miano V, Migliori V, Toolan-Kerr P, Sideri T, Enright AJ, et al. RNA modifications detection by comparative nanopore direct RNA sequencing. *Nat Commun*. 2021;12(1):7198.
- He PC, He C. m(6) A RNA methylation: from mechanisms to therapeutic potential. *Embo J*. 2021;40(3):e105977.

41. Mathlin J, Le Pera L, Colombo T. A census and categorization method of epitranscriptomic marks. *Int J Mol Sci* 2020, 21(13).
42. Tattoli I, Travassos LH, Carneiro LA, Magalhaes JG, Girardin SE. The nodosome: Nod1 and Nod2 control bacterial infections and inflammation. *Semin Immunopathol.* 2007;29(3):289–301.
43. Yang J, Pei G, Sun X, Xiao Y, Miao C, Zhou L, Wang B, Yang L, Yu M, Zhang ZS, et al. RhoB affects colitis through modulating cell signaling and intestinal Microbiome. *Microbiome.* 2022;10(1):149.
44. Ule J, Blencowe BJ. Alternative splicing regulatory networks: functions, mechanisms, and evolution. *Mol Cell.* 2019;76(2):329–45.
45. Pan Q, Shai O, Lee LJ, Frey BJ, Blencowe BJ. Deep surveying of alternative splicing complexity in the human transcriptome by high-throughput sequencing. *Nat Genet.* 2008;40(12):1413–5.
46. Su Z, Huang D. Alternative splicing of Pre-mRNA in the control of immune activity. *Genes (Basel)* 2021, 12(4).
47. Mellits KH, Mullen J, Wand M, Armbruster G, Patel A, Connerton PL, Skelly M, Connerton IF. Activation of the transcription factor NF-kappaB by *Campylobacter jejuni*. *Microbiol (Reading).* 2002;148(Pt 9):2753–63.
48. Lima SA, Chipman LB, Nicholson AL, Chen YH, Yee BA, Yeo GW, Collier J, Pasquinelli AE. Short poly(A) Tails are a conserved feature of highly expressed genes. *Nat Struct Mol Biol.* 2017;24(12):1057–63.
49. Dominissini D, Moshitch-Moshkovitz S, Schwartz S, Salmon-Divon M, Ungar L, Osenberg S, Cesarkas K, Jacob-Hirsch J, Amariglio N, Kupiec M, et al. Topology of the human and mouse m6A RNA methylomes revealed by m6A-seq. *Nature.* 2012;485(7397):201–6.
50. Meyer KD, Saletore Y, Zumbo P, Elemento O, Mason CE, Jaffrey SR. Comprehensive analysis of mRNA methylation reveals enrichment in 3'UTRs and near stop codons. *Cell.* 2012;149(7):1635–46.
51. Li B, Wang X, Li Z, Lu C, Zhang Q, Chang L, Li W, Cheng T, Xia Q, Zhao P. Transcriptome-wide analysis of N6-methyladenosine uncovers its regulatory role in gene expression in the lepidopteran *Bombyx Mori*. *Insect Mol Biol.* 2019;28(5):703–15.
52. Liu L, Zeng S, Jiang H, Zhang Y, Guo X, Wang Y. Differential m6A methylomes between two major life stages allows potential regulations in *trypanosoma brucei*. *Biochem Biophys Res Commun.* 2019;508(4):1286–90.
53. Zhou T, Chen G, Chen M, Wang Y, Zou G, Liang H. Direct Full-Length RNA sequencing reveals an important role of epigenetics during sexual reversal in Chinese Soft-Shell turtle. *Front Cell Dev Biol.* 2022;10:876045.
54. Russell KM, Smith J, Bremner A, Chintoan-Uta C, Vervelde L, Psifidi A, Stevens MP. Transcriptomic analysis of caecal tissue in inbred chicken lines that exhibit heritable differences in resistance to *Campylobacter jejuni*. *BMC Genomics.* 2021;22(1):411.
55. Shaughnessy RG, Meade KG, Cahalane S, Allan B, Reiman C, Callanan JJ, O'Farrelly C. Innate immune gene expression differentiates the early avian intestinal response between *Salmonella* and *Campylobacter*. *Vet Immunol Immunopathol.* 2009;132(2–4):191–8.
56. Shaughnessy RG, Meade KG, McGivney BA, Allan B, O'Farrelly C. Global gene expression analysis of chicken caecal response to *Campylobacter jejuni*. *Vet Immunol Immunopathol.* 2011;142(1–2):64–71.
57. Swaggerty CL, Pevzner IY, He H, Genovese KJ, Kogut MH. Selection for pro-inflammatory mediators produces chickens more resistant to *Campylobacter jejuni*. *Poult Sci.* 2017;96(6):1623–7.
58. Zhang M, Zhai Y, Zhang S, Dai X, Li Z. Roles of N6-Methyladenosine (m6A) in stem cell fate decisions and early embryonic development in mammals. *Front Cell Dev Biol.* 2020;8:782.
59. Cui X, Liang Z, Shen L, Zhang Q, Bao S, Geng Y, Zhang B, Leo V, Vardy LA, Lu T, et al. 5-Methylcytosine RNA methylation in *Arabidopsis thaliana*. *Mol Plant.* 2017;10(11):1387–99.
60. Yu F, Qi H, Gao L, Luo S, Njeri Damaris R, Ke Y, Wu W, Yang P. Identifying RNA modifications by direct RNA sequencing reveals complexity of epitranscriptomic dynamics in rice. *Genomics Proteom Bioinf.* 2023;21(4):788–804.
61. Motorin Y, Lyko F, Helm M. 5-methylcytosine in RNA: detection, enzymatic formation and biological functions. *Nucleic Acids Res.* 2010;38(5):1415–30.
62. Rice GI, Park S, Gavazzi F, Adang LA, Ayuk LA, Van Eyck L, Seabra L, Barrea C, Battini R, Belot A, et al. Genetic and phenotypic spectrum associated with IFIH1 gain-of-function. *Hum Mutat.* 2020;41(4):837–49.
63. Meng J, Yao Z, He Y, Zhang R, Zhang Y, Yao X, Yang H, Chen L, Zhang Z, Zhang H, et al. ARRDC4 regulates enterovirus 71-induced innate immune response by promoting K63 polyubiquitination of MDA5 through TRIM65. *Cell Death Dis.* 2017;8(6):e2866.

## Publisher's note

Springer Nature remains neutral with regard to jurisdictional claims in published maps and institutional affiliations.